Near-Field Gain of a Horn and an Open-Ended Waveguide: Comparison Between Theory and Experiment

MOTOHISA KANDA, SENIOR MEMBER, IEEE, AND R. DAVID ORR

Abstract—**Generating a standard electromagnetic field requires knowledge of the gain of the transmitting antenna. The theory and supporting experimental measurements of the near-field gain of a pyramidal horn and an open-ended waveguide (OEG) at 450 MHz are given. The empirical near-field gain for the OEG is derived from experimental results obtained by a two-antenna method at about 2 GHz. The theoretical near-field gain for the rectangular pyramidal horn is derived from Schelkunoff's formula. Two independent near-field gain measurements of these antennas are made using a three-antenna method and a transfer-standard-probe method. The discrepancy between theoretical and experimental results is typically less than ± 1 dB.**

I. INTRODUCTION

MICROWAVE ANECHOIC chambers are currently in use for a variety of indoor antenna measurements, electromagnetic interference (EMI) measurements, and electromagnetic compatibility (EMC) measurements. The prime requirement is that a transmitting antenna located within the chamber generate a known field throughout a volume (of the chamber) of sufficient size to perform antenna measurements. This volume is frequently referred to as a "quiet zone," and the level of interference between direct and reflected waves within it determines the performance of the anechoic chamber.

This paper is a status report on the evaluation of procedures for generating standard near fields in the National Bureau of Standards' (NBS) anechoic chamber (Fig. 1). Pyramidal horns or open-ended waveguides (OEG's) are used as transmitting antennas, positioned in the access doorway with their apertures inside the plane of the absorber points on the chamber wall.

Measurements in an anechoic chamber are usually performed in the near-field region of a standard transmitting antenna. The standard field on which these measurements are based is the radiated field intensity in the near-field region of this antenna. The antennas now used at NBS consist of a series of OEG's for frequencies below 500 MHz and a series of pyramidal horns above 500 MHz.

The field strength in an anechoic chamber is calculated at each frequency from power measurements. The value of standard field strength is given by the equation

$$E = \frac{\sqrt{30 p G_{\text{eff}}}}{d} \tag{1}$$

Manuscript received May 2, 1986; revised June 20, 1986.

The authors are with the Electromagnetic Fields Division, National Bureau of Standards, Boulder, CO 80303.

IEEE Log Number 8611098.

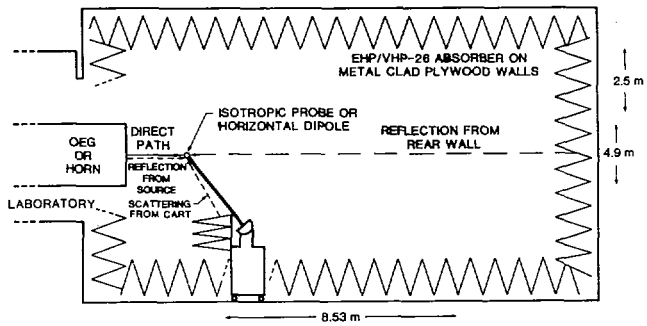

Fig. 1. Side view of the NBS-Boulder anechoic chamber.

where

- E on-axis magnitude of the electric field strength, V/m;
- p net power delivered to the standard transmitting horn or OEG, W;
- G_{eff} near-field power gain of the standard transmitting antenna, including near-field (proximity) correction factors; and
- d distance from the standard transmitting antenna aperture to the on-axis field point.

The approach used at NBS to measure accurately the net power delivered to a standard antenna involves the use of a four-port directional coupler with a standard mismatch and a 50-Ω matched termination. Details of the net power measurement are discussed elsewhere [1], [2].

Because an anechoic chamber is employed to generate standard electromagnetic fields computed from the near-field gain of a transmitting antenna, this paper discusses the theory and measurement of the near-field gain of a pyramidal horn and an OEG, and also the standard fields determined from those gains. First, the theoretical gain of a pyramidal horn is briefly reviewed [3]–[5]. An empirical equation giving the near-field gain of OEG's as a function of frequency and aperture dimensions is also given [6], [7].

Next, the experimental evaluation of the near-field gain of a pyramidal horn and an OEG is described. To obtain the near-field gain of both the horn and OEG simultaneously, the three-antenna and transfer-standard-probe measurements are performed at 450 MHz. This frequency is within the range of both the horn and OEG, and gives the same transfer-standard-probe response (Fig. 7) as does the 100-MHz calibration frequency. In the three-antenna technique, we use a microstrip patch antenna and a 500-MHz resonant dipole, as well as a horn or

an OEG. In the transfer-standard-probe technique, an electrically short dipole antenna is typically used (e.g., the NBS electric-field monitors EFM-3 or EFM-5 [8], [9]). This probe is often calibrated in a transverse electromagnetic (TEM) cell and therefore has a known response over a given range of frequency and amplitude. The near-field gains of the pyramidal horn and the OEG that are determined by use of the three-antenna technique and the transfer-standard-probe technique are compared with the theoretically determined near-field gains of these antennas.

II. Near-Field Gain Calculations for a Rectangular Pyramidal Horn and an Open-Ended Rectangular Waveguide

The EM field measurements in an anechoic chamber are usually performed in the near-field region of the standard transmitting antenna where calculated values for the field intensity constitute the known standard field. The antennas employed for this purpose are OEG's below 500 MHz and pyramidal horns above 500 MHz.

A. Pyramidal Horn

The approach used at NBS to establish a standard field at frequencies above 500 MHz employs a series of pyramidal horns. In deriving the gain of a pyramidal horn by the Kirchhoff method, Schelkunoff accounted for the effect of horn flare by introducing a quadratic phase error in the dominant mode field along the aperture coordinates [3]. The geometrical optics description of single diffraction by the aperture edges yields essentially the Kirchhoff results. The proximity effect in the near field can also be approximated by a quadratic phase error in the aperture field [4].

To improve Schelkunoff's gain equation, Jull [10] used the geometric theory of diffraction to include reflection of the diffracted fields from the horn interior and double diffraction at the aperture in his analysis of the on-axis near-field gain of an E-plane sectoral horn. The resulting near-field gain of a pyramidal horn is

$$G=\frac{32ab}{\pi\lambda^2}R_E R_H, \tag{2}$$

where R_E and R_H are the gain reduction factors due to E-plane and H-plane flares, respectively. The pertinent horn dimensions used in (2) are shown in Fig. 2. The factor $32\,ab/(\pi\lambda^2)$ is the far-field gain of a rectangular aperture with an in-phase field distribution uniform across one dimension and cosinusoidal across the other.

The H-plane factor R_H is given by [10]

$$R_H=\frac{\pi^2\{[C(u)-C(v)]^2+[S(u)-S(v)]^2\}}{4(u-v)^2}, \tag{3}$$

where C and S are the Fresnel integrals defined as

$$C(w)-jS(w)=\int_0^w \exp\,(-j\pi t^2/2)\,dt, \tag{4}$$

and their arguments u and v are defined as

$$u=A+B,\quad v=-A+B,$$

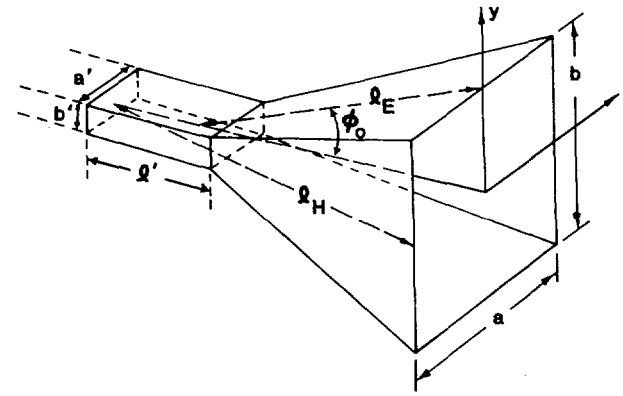

Fig. 2. Dimensions of a pyramidal standard gain horn.

with

$$A=\frac{a}{(2\lambda l'_H)^{1/2}},\quad B=\frac{1}{a}(\lambda l'_H/2)^{1/2},$$

$$l'_H=rl_H/(r+l_H) \tag{5}$$

and r being the distance between the center of the horn aperture and the field point.

The E-plane factor R_E is given by [10]:

$$R_E=\frac{1}{w^2(1+\cos\,\phi_0)}\left|\exp\,(-jkl'_E\,\cos\,\phi_0)\right.$$
$$\left.+2v(l'_E,\ \pi-\phi_0)+\frac{\pi a'}{a}S_2\right|^2, \tag{6}$$

where

$$w=\frac{b}{(2\lambda l'_E)^{1/2}\cos\,(\phi_0/2)},\quad \text{and } l'_E=rl_E/(r+l_E) \tag{7}$$

and ϕ_0 is half the E-plane flare angle. For any two variables l and ψ, the factor $v(l,\ \psi)$ is given by

$$v(l,\ \psi)=-\frac{\exp\,(jkl\,\cos\,\psi)}{2}[1-(1+j)D], \tag{8}$$

with

$$D=C[(4kl/\pi)^{1/2}\cos\,(\psi/2)]-jS[(4kl/\pi)^{1/2}\cos\,(\psi/2)]. \tag{9}$$

The factor S_2 is defined as

$$S_2=\sum_{i=1}^{m} v\left(l'_E,\ \frac{\pi}{2}-i\phi_0\right)f\left(d_i,\ \pi-\phi_0,\ \frac{\pi}{2}-i\phi_0\right), \tag{10}$$

where

$$f(d,\ \theta,\ \theta_0)=v(d,\ \theta-\theta_0)+v(d,\ \theta+\theta_0). \tag{11}$$

$d_i = 2l\,\sin\,(i\phi_0)$ is the ray-path length between single and double diffraction, and m is the largest integer less than $\pi/2\phi_0$.

Neglecting the diffracted fields of the aperture edge

reflected from the horn interior (term S_2 in (6)), and assuming a small flare angle such that $\phi_0 \approx b/2l$, one can show that the E-plane factor can be simplified as

$$R_E = \frac{C^2(w) + S^2(w)}{w^2}, \tag{12}$$

where

$$w = \frac{b}{\sqrt{2\lambda l'_E}}. \tag{13}$$

When R_E and R_H are given by (12) and (3), (2) is the well-known Schelkunoff–Braun expression for the gain of a pyramidal horn. In Section IV-A, we show that (12) gives a much better representation of our near-field horn gain data than (6), and therefore in (6) we neglect the S_2 diffraction term developed in [10]. Equation (6) then reduces to (12).

Simple polynomial expressions for (3) and (12) have been generated for the near-field gain-reduction factors, R_H and R_E, for pyramidal horns [11]. The value of these gain-reduction factors depends on frequency, horn dimensions, and distance to the on-axis field point. The two gain-reduction factors, R_H and R_E, are given in dB by

$$R_H = (0.01\alpha)(1 + 10.19\alpha + 0.51\alpha^2 - 0.097\alpha^3)$$
$$R_E = (0.1\beta^2)(2.31 + 0.053\beta), \tag{14}$$

where

$$\alpha = \left(\frac{a^2F}{0.3}\right)\left[\frac{1}{l_H} + \frac{1}{r}\right] \text{ and } \beta = \left(\frac{b^2F}{0.3}\right)\left[\frac{1}{l_E} + \frac{1}{r}\right].$$

F is frequency, GHz.

The theoretical gain of the horn, near field or far field, is then given by

$$\text{gain} = (113.3abF^2)[10^{-(R_H + R_E)/10}],$$

or

$$\text{gain (dB)} = 10 \log (ab) + 20 \log F + 20.54 - R_H - R_E. \tag{15}$$

The near-field gain ((2)) of a pyramidal horn is then used to calculate the radiated field intensity in the near field of the antenna. For the horn used in our measurements at 450 MHz, the gain reduction factors R_E and R_H expressed in decibels are shown in Fig. 3. The effectiveness of these correction factors is determined by comparing theoretical gain values with experimental results.

B. Open-Ended Waveguide

Early work to determine the field pattern and gain of large OEG radiators, both theoretically and experimentally, is described in [7]. An equation giving the gain of OEG's as a function of frequency and aperture dimensions has been determined experimentally at NBS. The original data for this equation come from a two-antenna calibration using two

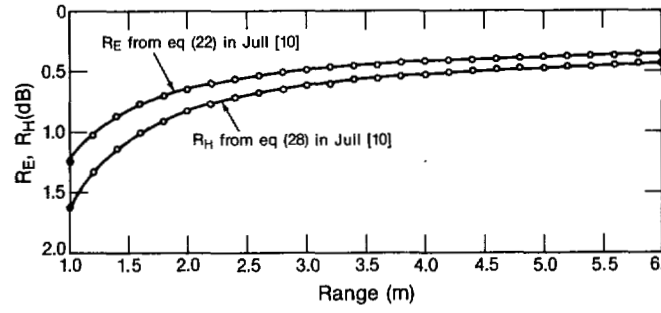

Fig. 3. Gain reduction factors R_E and R_H for the standard gain horn at 450 MHz.

identical open-ended guides [6]. The apertures of the OEG's used at NBS have a two-to-one aspect ratio. In this case, the equation for calculating the antenna gain is

$$\text{gain} = 21.6 \text{ Fw},$$

or

$$\text{gain (dB)} = 10 \log (\text{Fw}) + 13.34 \tag{16}$$

where F is frequency, GHz, and w is width (larger side) of the two-to-one OEG, m.

At present there is no complete, rigorous theory of OEG near-field gain, though the following analysis has been suggested by Yaghjian [12]. The near-field gain of an open-ended, unflanged rectangular waveguide can be calculated from the forward near-field power pattern, which is determined from the conventional far-field power pattern by use of the plane wave scattering theorem [13].

The geometry of the open-ended rectangular waveguide is shown in Fig. 4. The far-field E-plane pattern, $E_E(\theta)$, is predicted quite accurately by inserting the electric and magnetic fields of the propagating TE_{10} mode into the Stratton–Chu formula and integrating over the aperture of the waveguide [14]. Thus we have

$$E_E(\theta) = A_E \frac{\{1 + (\beta/k)\cos\theta + \Gamma[1 - (\beta/k)\cos\theta]\}}{[1 + \beta/k + \Gamma(1 - \beta/k)]} \cdot \frac{\sin[(kb/2)\sin\theta]}{(kb/2)\sin\theta} \tag{17}$$

where the normalized propagation constant β/k for the TE_{10} mode equals $[1 - (\pi/ka)^2]^{1/2}$, with k being the free space wavenumber, and Γ is the reflection coefficient of the TE_{10} mode at the end of the waveguide. The constant A_E, which is related to the amplitude of the incident TE_{10} mode, will be defined later.

In the case of the H-plane fields, the aperture integration of the Stratton–Chu formulas with the electric and magnetic fields of the TE_{10} mode neglects the "fringe" currents and, therefore, produces much too broad an H-plane pattern. Using an estimate of the fringe currents on the $x \pm a/2$ sides of the rectangular waveguide from a numerical solution to the electric-field integral equation applied to the open-ended rectangular waveguide [15], we obtain for the far-field H-

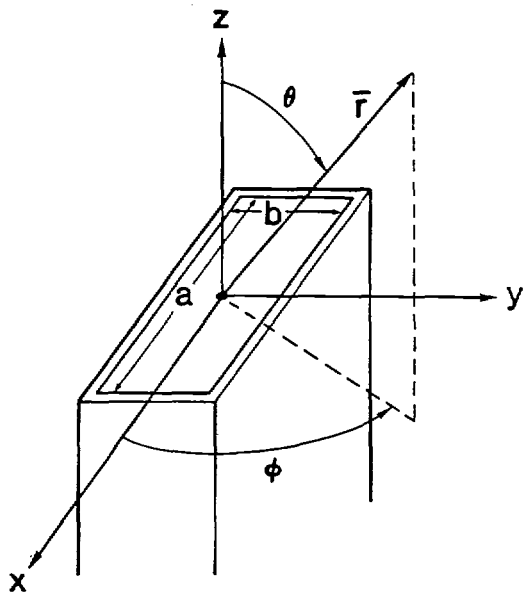

Fig. 4. Aperture dimensions and field coordinate system for an open-ended waveguide.

plane pattern

$$E_H(\theta)=A_H\left[\frac{(\cos\theta+\beta/k)+\Gamma\ (\cos\theta-\beta/k)}{(\pi/2)^2-[(ka/2)\ \sin\theta/2]^2}+C_0\right]\cdot\cos\left(\frac{ka}{2}\sin\theta\right). \quad (18)$$

The constant A_H is related to A_E by

$$A_E=A_H\{(2/\pi)^2[1+\beta/k+\Gamma(1-\beta/k)]+C_0\}. \quad (19)$$

The constant C_0 is calculated by equating the radiated power determined from the far field to the total input power determined from the TE_{10} mode field.

From (17), (18), and (19) for the OEG far field, the plane-wave scattering theorem [13] will yield near-field expressions from which the near-field power density can be obtained (and thence the OEG gain with respect to an isotropic radiator). In a future publication we will present this analysis and a comparison of the resulting expression for OEG near-field gain with measured gain values. The evaluation of the uncertainty of the near-field gain will be performed by comparing it with the experimental results.

III. Experiments

To evaluate the near-field gain of a pyramidal horn and an OEG, we have used the three-antenna technique and the transfer-standard-probe technique which are briefly described below.

A. Three-Antenna Technique

By measuring the power transfer between each pair of three antennas separated by a distance r, we can determine the near-field gains of the three antennas from three power transmission equations:

$$\frac{P_i^r}{P_j^t}=\left(\frac{\lambda}{4\pi r}\right)^2 G_i^{\text{eff}}(r)\cdot G_j^{\text{eff}}(r) \quad (20)$$

where

P^r	available power from a receiving antenna,
P^t	net power delivered to a transmitting antenna,
$G^{\text{eff}}(r)$	near-field gain of a receiving (i) or transmitting (j) antenna at a distance r from that antenna, and
i, j	1, 2, and 3 ($i \neq j$).

For example, the near-field gain of a number 1 antenna can be obtained by

$$G_1^{\text{eff}}(r)=\frac{4\pi r}{\lambda}\left[\frac{P_1^r}{P_2^t}\cdot\frac{P_3^r}{P_1^t}\cdot\frac{P_3^t}{P_2^r}\right]^{1/2}. \quad (21)$$

This expression is rigorous only for point sources and receivers. The horn, OEG, and patch antennas employed in our gain measurements all have large apertures, and the 500 MHz half-wave dipole has a span of 15 cm. Thus, the transmission path between each pair of antennas is a composite of the paths from each point of the transmitting aperture to every point of the receiving aperture. Therefore, the data we present as boresight gains are averages resulting from the transmission distributed over each pair of finite apertures. This effect will contribute to the discrepancy between our measured and computed gains.

For the near-field gain measurements of a pyramidal horn at 450 MHz, we use a standard gain horn which has the following dimensions: a = 122.5 cm, b = 90.75 cm, l_H = 142.0 cm, and l_e = 121.3 cm. For the near-field gain measurements of an OEG at 450 MHz, we use a specially fabricated OEG which has an aperture of 53.34 × 26.67 cm (21 × 10.5 in) and a length of about 2 m. In the three-antenna technique, a square microstrip antenna and a dipole antenna are used as well as a rectangular horn or an OEG. The square microstrip antenna (Fig. 5) used in the experiments has a coaxial line feed and is resonant at 450 MHz. Details of the theory and experimental evaluation of the microstrip antenna are given elsewhere [16]. The 30-cm dipole antenna used in the experiment is resonant at about 500 MHz. The dipole is terminated with two 50-Ω loads, one of which is a power meter as shown in Fig. 6. Thus, the total power received by the dipole antenna is twice the reading of the power meter.

B. Transfer-Standard-Probe Technique

We have developed various kinds of electrically small dipoles for sensing E-fields and electrically small loops for H-fields. These probes have a known response over a given range of frequency and amplitude [8], [17]. Such a probe antenna can be used to measure and verify field strength as a function of distance from a transmitting antenna. In this application, the probe serves as a transfer standard and must be calibrated by an independent approach over the same frequency and amplitude range. We use a TEM transmission line cell for establishing standard EM fields [18]. For the single-frequency data reported here, the transfer-standard

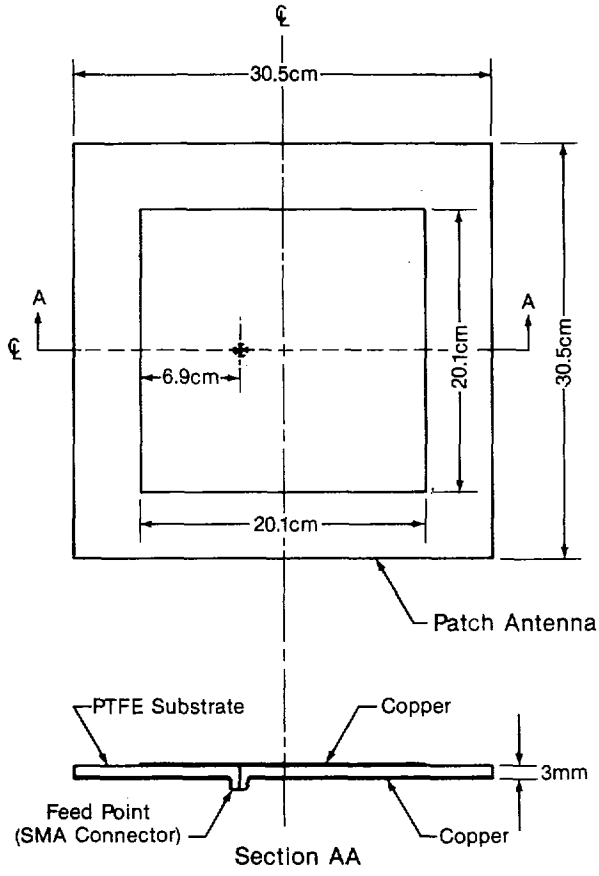

Fig. 5. Construction and dimensions of the square microstrip patch antenna.

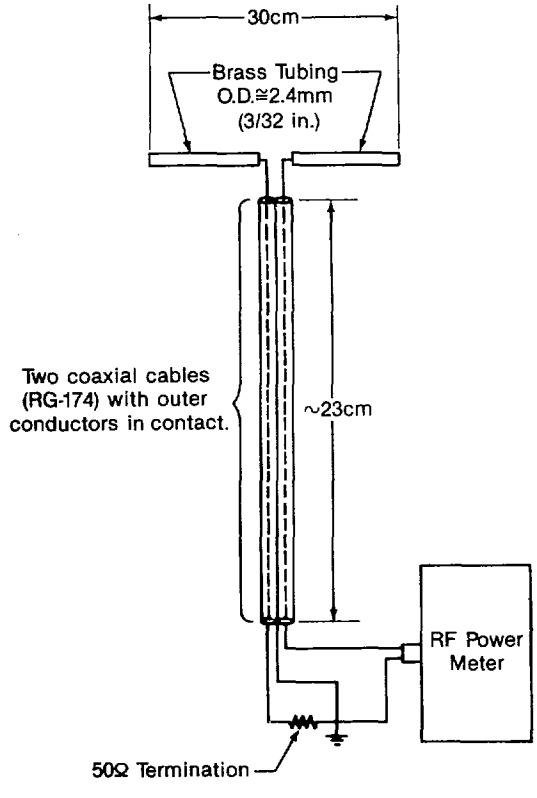

Fig. 6. The 30-cm dipole employed in three-antenna gain measurements.

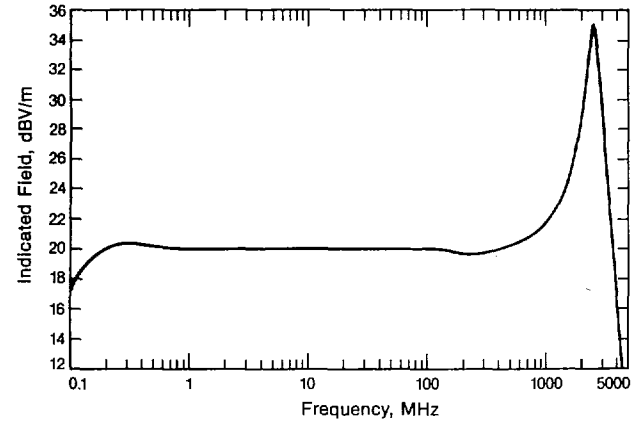

Fig. 7. Typical response of an EFM-5 probe vs frequency in a 10 V/m field.

electric field probes (such as EFM-3 or EFM-5) are calibrated for dynamic range at 100 MHz using a TEM cell. The frequency response of these transfer probes is well established over the range between 500 kHz and 1 GHz and is shown in Fig. 7. In another method, we obtain antenna near-field gain vs distance by adjusting the power delivered to the transmitting antenna to keep a constant output voltage from the probe as it scans the antenna near field. In this way the field strength at the probe is held constant, the probe requires calibration at only one dynamic level, and nonlinearity in the probe response vs dynamic range can be ignored. The transmitted power required to obtain this constant response is recorded as a function of separation distance between the transmitting antenna and receiving probe. Then, from the transmitted power measured vs distance, the near-field gain reduction of the antenna can be evaluated.

IV. Near-Field Gain Evaluation

This section discusses the near-field gain of the pyramidal horn and the rectangular OEG. The near-field gain that is computed from the theory described in Section II is compared with the experimental results obtained by the techniques given in Section III.

A. Pyramidal Horn

The standard pyramidal horn used in this study has the following measured dimensions: a = 122.5 cm, b = 90.75 cm, l_H = 142.0 cm, and l_E = 121.3 cm. The range dependence of the theoretical and measured gain of this horn is shown in Fig. 8. The theoretical near-field gain ((3) and (12) in (2)) does not include the gain reduction due to multiple diffraction and diffracted fields reflected from the horn interior. The discrepancy between theoretical and experimental near-field gain of the horn is typically 0.6 dB. As a function of distance from the horn aperture, the experimental near-field gain curve is not monotonic, as is predicted by the theory, but shows definite quasiperiodic wiggles. This effect can probably be attributed to multiple reflections between the horn and the other two antennas, particularly the patch antenna, employed in the three-antenna measurement method. The theory, which takes into account the reflection of diffracted fields from the horn interior and double diffraction at the aperture (given in

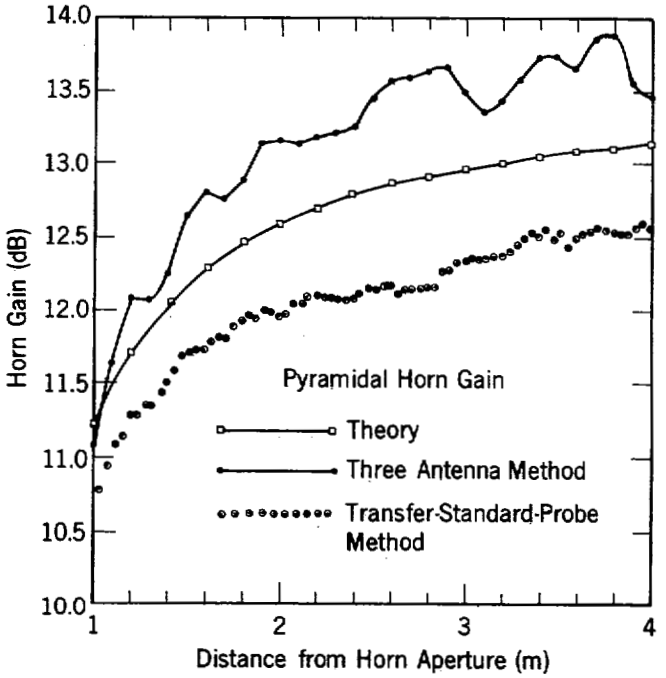

Fig. 8. Range dependence of the pyramidal horn gain at 450 MHz.

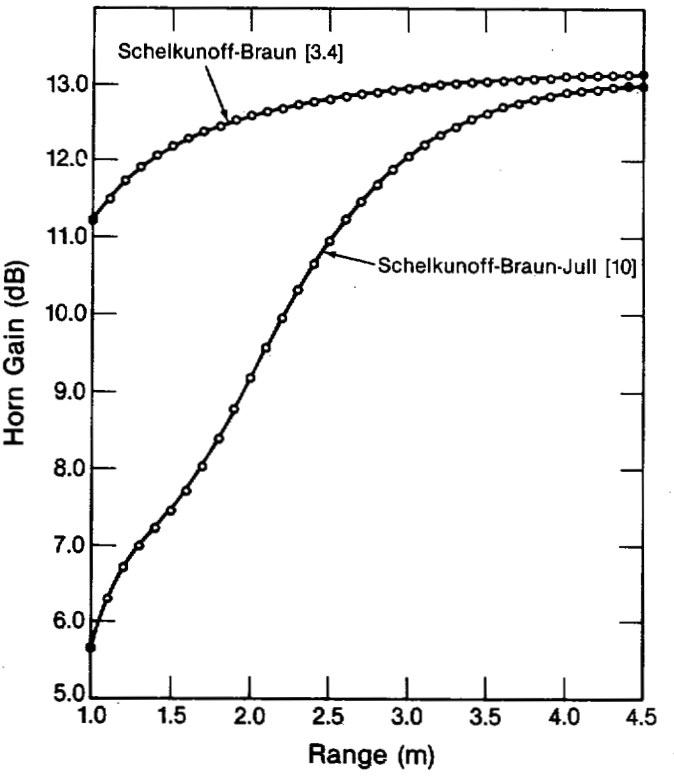

Fig. 9. Near-field horn gain at 450 MHz with and without the Jull diffraction term S_2 in (6).

Section II), has been examined without much success. Fig. 9 shows the near-field horn gain computed using (6) and (12) for R_E in (2). In the 1–2 m range, the diffraction analysis [10] represented by term S_2 in (6) predicts a near-field gain reduction of 3–5 dB in addition to that affected by (12). The ~0.6-dB discrepancy between the Schelkunoff–Braun data and our measured gain values therefore motivated our use of (12) for R_E.

The near-field gain of the pyramidal horn is also examined using the electrically short dipole probe. The electric field probe is calibrated independently using a TEM cell. Fig. 10 shows the electric field strength from the horn whose net delivered power is set at 1 W. Theoretical electric field strength is derived using the near-field horn gain calculated from the Schelkunoff–Braun theory described in Section II. Experimental electric field strength is derived using the near-field horn gain obtained by the three-antenna measurements. The electric field strength measured by the transfer-standard probe is typically 0.5 dB lower than the theoretically predicted values, whereas the electric field computed from horn gain values measured by the three-antenna method is typically 0.6 dB higher than the theoretically predicted values.

The discrepancy between the theoretical electric field strength and experimental electric field strength (the latter obtained by two independent techniques: the three-antenna method and the transfer-standard-probe method) can be attributed to many assumptions to simplify the theory. For example, the theory does not take into account multiple diffraction and diffracted fields reflected from the horn interior and the possible higher modes in the horn aperture. An improved theory that includes these effects will be a future topic of study.

In the three-antenna gain measurements, multiple reflections between the horn and the other two antennas (particularly

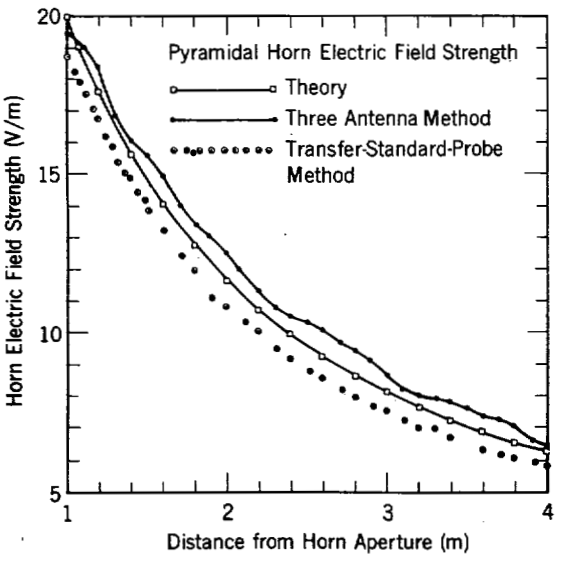

Fig. 10. Pyramidal horn electric field strength (1 W delivered power; 450 MHz).

the patch antenna because of its large dimensions) have affected the near-field horn measurements. At the same time, since the transfer-standard-probe (EFM-5) is calibrated using a TEM cell, loading of the cell [18] due to the presence of the 5-cm dipole probe has caused some calibration error.

B. Open-Ended Waveguide

The OEG used in this study has an aperture of 53.34 × 26.67 cm (21 × 10.5 in). The near-field gain of the OEG is calculated by the empirical equation given in Section II. The

experimental near-field gain of this OEG is independently obtained using the three-antenna technique and the transfer-standard-probe method. In the three-antenna method, the patch antenna, resonant at 450 MHz, and a 30-cm dipole antenna are used with the OEG.

Fig. 11 shows the near-field gain of the OEG obtained from the (empirical) theory, the three-antenna method, and the transfer-standard-probe method. The large gain reduction of about 0.5 dB at around three meters distance from the aperture can probably be attributed to higher modes excited in the waveguide interior. The discrepancy between the (empirical) theory ((16)) and the three-antenna method is typically about 0.5 dB, and ranges from -0.4 dB to -1 dB between the two experimental curves.

In Fig. 12, we compare the theoretical and two experimental sets of OEG data by plotting the electric field computed from each data set for 1 W net power to the OEG. The theoretical electric field strengths are derived using the (empirical) theoretical gain ((16)) given in Section II. The electric field strength obtained by the three-antenna method is computed using the near-field gain obtained by the three-antenna method and shown in Fig. 11. The electric field strength obtained by the transfer-standard-probe method for a known net power to the OEG is scaled to 1 W delivered power. In Fig. 12, the theoretical field strength is about 0.7 dB higher than the three-antenna method results, whereas the transfer-standard field measurements are about 0.8 dB lower than the electric field strengths computed from three-antenna method gain values. (As mentioned in Section II-B, (16) giving the near-field gain of the OEG was determined empirically from a two-antenna calibration method using two identical OEG's. An improved expression for near-field OEG gain will be derived from near-field expressions obtained from the theoretical far field ((17)–(19)) by use of the plane wave scattering theorem. This work will be reported in a later publication.) In the three-antenna calibration method, multiple reflections between the OEG and the microstrip patch antenna might have perturbed the transmitted field and introduced error into measured gain values. In the transfer-standard-probe method, the loading effect due to the presence of the transfer-standard probe in a TEM cell causes some error in the probe calibration.

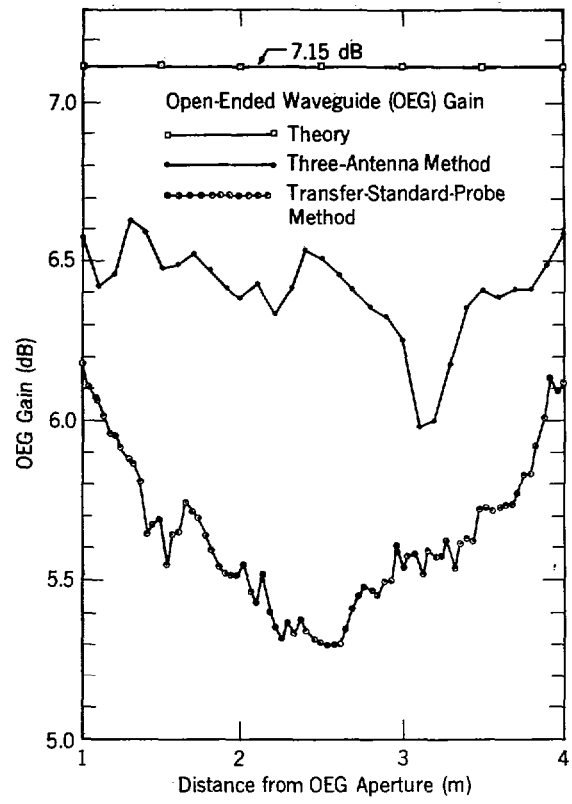

Fig. 11. Range dependence of the open-ended waveguide gain at 450 MHz.

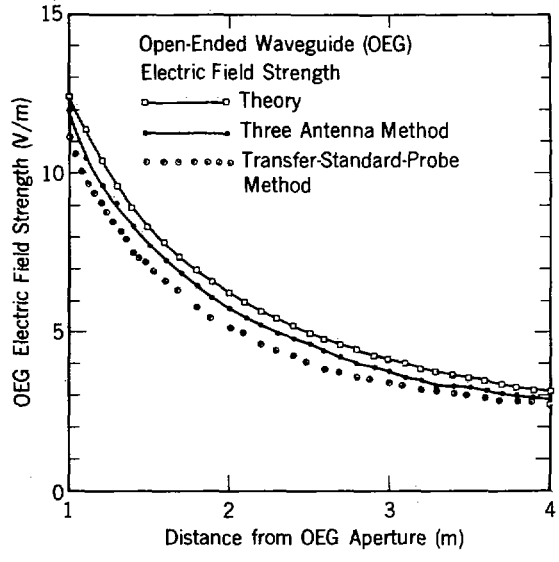

Fig. 12. Open-ended waveguide electric field strength (1 W delivered power; 450 MHz).

V. Conclusion

Using a three-antenna method, we have evaluated the near-field gain of a horn and an OEG at 450 MHz. In the three-antenna method, we have used a microstrip patch antenna and a 500-MHz resonant dipole antenna along with the horn or OEG that is to be evaluated. To further evaluate the near-field gain of antennas, we have used NBS transfer-standard probes calibrated in a TEM cell. These experimental near-field gains are compared with theoretical results.

For the horn antenna used in the experiments, the discrepancy between 1) the near-field gain measured by the three-antenna method, and 2) that measured by a transfer-standard probe is about 1 dB for the distance of 1-4 m from the horn aperture. The theoretical curve for near-field gain lies midway between both sets of experimental gain measurements. The discrepancy between the OEG theoretical (empirical) near-field gain and the experimental near-field gain of the three-antenna measurements is about 0.5 dB, whereas the discrepancy between the theory and the transfer-standard-probe measurement ranges from -1 dB to -1.7 dB.

The discrepancies between the three-antenna and transfer-standard data indicate the difficulty of generating standard near fields in the anechoic chamber, and alert one to the greater uncertainties encountered in near-field measurements. Further work will attempt to resolve these discrepancies.

REFERENCES

[1] M. Kanda and R. D. Orr, "A radio-frequency power delivery system: procedures for error analysis and self-calibration," Nat. Bur. Stand. Tech. Note 1083, Aug. 1985.

[2] R. W. Beatty and A. C. MacPherson, "Mismatch errors in microwave power measurements," *Proc. IRE,* vol. 41, no. 9, pp. 1112–1119; Sept. 1953.

[3] S. A. Schelkunoff and H. T. Friis, *Antennas, Theory and Practice.* New York: Wiley, 1952.

[4] E. H. Braun, "Gain of electromagnetic horns," *Proc. IRE,* vol. 41, no. 1, pp. 109–115; Jan. 1953.

[5] E. V. Jull, "Finite-range gain of sectoral and pyramidal horns," *Electron. Lett.,* vol. 6, pp. 680–681, 1970.

[6] R. R. Bowman, "Calibration techniques for electromagnetic hazard meters: 500 MHz to 20 GHz," Nat. Bur. Stand. NBSIR 75-805, Apr. 1976.

[7] W. L. Barrow and F. M. Greene, "Rectangular hollow-pipe radiators," *Proc. IRE,* vol. 26, no. 12, pp. 1498–1590, Dec. 1938.

[8] E. B. Larsen and F. X. Ries, "Design and calibration of the NBS isotropic electric-field monitor," Nat. Bur. Stand. (U.S.) Tech. Note 1033, Mar. 1981.

[9] M. Kanda, "Analytical and numerical techniques for analyzing an electrically short dipole with a nonlinear load," *IEEE Trans. Antennas Propagat.,* vol. AP-28, pp. 71–78; Jan. 1980.

[10] E. V. Jull, "Errors in the predicted gain of pyramidal horns," *IEEE Trans. Antennas Propagat.,* vol. AP-21, pp. 25–31, Jan. 1973.

[11] E. B. Larsen, "Techniques for producing standard EM fields from 10 kHz to 10 GHz for evaluating radiation monitors," in *Proc. Symp. Electromagn. Fields in Biologic. Syst.,* S. S. Stuchly, Ed., Ottawa, Canada, June 27–30, 1978. Canada: Int. Microwave Power Inst., 1979, pp. 96–112.

[12] A. D. Yaghjian, "Efficient computation of antenna coupling and fields within the near-field region," *IEEE Trans. Antennas Propagat.,* vol. AP-30, pp. 113–128, Jan. 1982.

[13] D. M. Kerns, "Plane-wave scattering-matrix theory of antennas and antenna-antenna interactions," Nat. Bur. Stand. Monogr. 162, June 1981.

[14] J. A. Stratton, *Electromagnetic Theory.* New York: McGraw-Hill, 1941.

[15] A. D. Yaghjian, "Approximate formulas for the far fields and gain of open-ended rectangular waveguide," Nat. Bur. Stand. NBSIR 83-1689; May 1983.

[16] M. Kanda, "Rectangular microwave patch antenna as a standard for generating electromagnetic fields," to be published.

[17] L. D. Driver and J. E. Cruz, "Development of the NBS isotropic magnetic-field meter [MFM-10], 300 kHz to 100 MHz," presented at 1982 IEEE Int. Symp. Electromagn. Compat., Santa Clara, CA.

[18] M. Kanda, E. B. Larsen, M. Borsero, P. G. Galliano, I. Yokoshima, and N. S. Nahman, "Standards for electromagnetic field measurements," *Proc. IEEE,* vol. 74, no. 1, pp. 120–128, Jan. 1986.

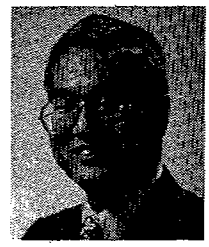

Motohisa Kanda (S'67–M'68–SM'83) received the B.S. degree from Keio University, Toyko, Japan, in 1966, and the M.S. and Ph.D. degrees in electrical engineering from the University of Colorado, Boulder, in 1968 and 1971, respectively.

From 1965 to 1966 he did research on the avalanche breakdown in germanium p-n junction at a cryogenic temperature at Keio University. From 1966 to 1971 he was a Research Assistant at the University of Colorado, where he was engaged in the research on impact ionization of impurities in n-type germanium, and nonreciprocal behavior in solid-state magnetoplasma at millimeter and submillimeter wavelengths. In 1971 he joined the National Bureau of Standards, Boulder, Colorado, where he is currently Group Leader of the Fields Characterization Group of the Electromagnetic Fields Division. Concurrently he has been an Adjoint Professor in the Electrical Engineering Department of the University of Colorado, Boulder.

Dr. Kanda is a full member of Commissions A, B, and E of the International Union of Radio Science and Sigma Xi.

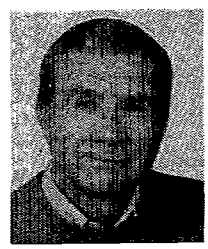

R. David Orr received the B.S. degree from Kalamazoo College, Kalamazoo, MI, in 1950, and the M.S. and Ph.D. degrees from the University of Colorado, Boulder, in 1960 and 1971, respectively, all in physics.

He worked as a heat treating engineer at the Western Electric Company, Cicero, IL, and continued as a Physicist in the Particle Accelerator Division of Argonne National Laboratory, Lemont, IL. After several years in a nutrient matrix of Army service, graduate school, science journalism, and teaching physics at San Jose State College, San Jose, CA, he emerged in 1979 as a Physicist at the National Bureau of Standards, Boulder, CO. His current assignment is to evaluate the pyramidal horns and anechoic chamber employed by NBS to establish standard radio-frequency fields in which calibrations and electromagnetic susceptibility measurements are made.